Markedly Enhancing Enzymatic Enantioselectivity in Organic Solvents by Forming Substrate Salts

Tao Ke and Alexander M. Klibanov*

Contribution from the Department of Chemistry, Massachusetts Institute of Technology, Cambridge, Massachusetts 02139

Received December 11, 1998

Abstract: A new approach is proposed to enhance enzymatic enantioselectivity in organic solvents. It is based on the presumption that the less reactive substrate enantiomer experiences greater steric hindrances in the enzyme-bound transition state than the more reactive one; enlarging the substrate by forming a salt with a bulky counterion should exacerbate these hindrances disproportionately for the less reactive enantiomer, thus increasing the enantioselectivity. This strategy was implemented and verified with several structurally diverse chiral compounds converted to salts by treatment with numerous Brønsted−Lowry acids or bases. Enzymatic transesterifications or hydrolyses of the resultant racemic salts were much more enantioselective than those of the free substrates. This effect was observed in various organic solvents (but not in water, where the salts apparently dissociate to regenerate the free substrates), using both crystalline and lyophilized enzymes (*Pseudomonas cepacia* lipase and the protease subtilisin Carlsberg). As demonstrated both analytically and preparatively, in some instances an enzyme would exhibit virtually no enantiopreference toward a free substrate but a profound one toward its salts. All these effects were rationalized by using molecular modeling to derive enzyme-bound transition-state structures of *R* and *S* enantiomers of both free substrates and their salts. The areas of substrate surfaces overlapping with the enzyme calculated from these models turned out to be a remarkably good predictor of enzymatic enantioselectivity (*E*)—the greater the difference in the area of surface overlap between the enantiomers, the higher the *E* value.

Introduction

Spurred by the ever-growing demand for enantiopure pharmaceuticals,[1] as well as agricultural and other specialty chemicals, the use of enzymes as asymmetric practical catalysts continues to expand.[2] A major obstacle to this expansion is that an enzyme from a given source is often insufficiently enantioselective toward a particular (e.g., commercially valuable) substrate, thus leading to its incomplete enzymatic resolution and a poor e.e. of the resultant product.[3] A traditional remedy for this problem is to screen enzymes from other sources in the hope of finding a more enantioselecive one.[4] This empirical and laborious approach is unappealing to organic chemists, and therefore alternative strategies have been sought. Among such means[3,5] identified to manipulate enzymatic enantioselectivity, temperature[6] and, in the case of nonaqueous enzymology,[7] solvent[8] are notable for their broad applicability.

The realization that enzymes can function in organic solvents and the current widespread use of this phenomenon[7] have offered novel opportunities for improving enzymatic enantioselectivity. For example, in addition to the aforementioned solvent control of enzyme enantioselectivity,[8] the latter is also a function of enzyme history.[9] In this study, we propose a new strategy for increasing the enantioselectivity of enzymes in organic solvents. It is based on the idea that discrimination between the two substrate enantiomers by a given enzyme can be enhanced by temporarily enlarging the substrate via salt formation. A bulky counterion in such a salt will exacerbate the steric hindrances encountered by the less reactive (and hence more sterically constrained) substrate enantiomer in the enzyme-bound transition state, thus increasing the enantioselectivity E[10] and, in turn, product e.e. Following the enzymatic resolution and enzyme removal, the reaction mixture is separated and treated with an acid or base to dissociate the salt and recover the free substrate and product.

Results and Discussion

Our overall goal is to discover and exploit new, facile approaches to enhancing the enantioselectivity of a given

(1) Stinson, S. C. *Chem. Eng. News* **1998**, *76*, No. 38.
(2) Sheldon, R. A. *Chirotechnology: Industrial Synthesis of Optically Active Compounds*; M. Dekker: New York, 1993. Wong, C.-H.; Whitesides, G. M. *Enzymes in Synthetic Organic Chemistry*; Pergamon Press: Oxford, 1994. Drauz, K.; Waldmann, H. *Enzyme Catalysis in Organic Synthesis*, 2nd ed.; Springer-Verlag: Berlin, 1996. Zaks, A.; Dodds, D. R. *Drug Dev. Trends* **1997**, *2*, 513−531. Faber, K. *Biotransformations in Organic Chemistry*, 3rd ed.; Springer-Verlag: Berlin, 1997.
(3) Faber, K.; Ottolina, G.; Riva, S. *Biocatalysis* **1993**, *8*, 91−132.
(4) Roberts, S. M.; Turner, N. J.; Willetts, A. J.; Turner, M. K. *Introduction to Biocatalysis Using Enzymes and Microorganisms*; Cambridge University Press: New York, 1995.
(5) Chen, C.-S.; Sih, C. J. *Angew. Chem., Ind. Ed. Engl.* **1989**, *28*, 695−707. Hult, K.; Norin, T. *Pure Appl. Chem.* **1992**, *64*, 1129−1134.
(6) Phillips, R. S. *Trends Biotechnol.* **1996**, *14*, 13−16.
(7) Koskinen, A. M. P.; Klibanov, A. M., Eds. *Enzymatic Reactions in Organic Media*; Blackie: London, 1996.
(8) Wescott, C. R.; Klibanov, A. M. *Biochim. Biophys. Acta* **1994**, *1206*, 1−9. Carrea, G.; Ottolina, G.; Riva, S. *Trends Biotechnol.* **1995**, *13*, 63−70. Wescott, C. R.; Noritomi, H.; Klibanov, A. M. *J. Am. Chem. Soc.* **1996**, *118*, 10365−10370.
(9) Stahl, M.; Jeppsson-Wistrand, U.; Mansson, M.-O.; Mosbach, K. *J. Am. Chem. Soc.* **1991**, *113*, 9366−9368. Noritomi, H.; Almarsson, Ö.; Barletta, G. L.; Klibanov, A. M. *Biotechnol. Bioeng.* **1996**, *51*, 95−98. Ke, T.; Klibanov, A. M. *Biotechnol. Bioeng.* **1998**, *57*, 746−750.
(10) Chen, C.-S.; Fujimoto, Y.; Girdaukas, G.; Sih, C. J. *J. Am. Chem. Soc.* **1982**, *104*, 7294−7299. Straathof, A. J. J.; Jongejan, J. A. *Enzyme Microb. Technol.* **1997**, *21*, 559−571.

10.1021/ja984283v CCC: $18.00
Published on Web 03/17/1999

Table 1. Enantioselectivity of Cross-Linked Crystalline *Pseudomonas cepacia* Lipase toward **1** and Its Salts with Various Carboxylic Acids in the Transesterification Depicted in Scheme 1 in Different Anhydrous Solvents and in the Hydrolysis in Water[a]

	E (*S*/*R*)				
substrate	acetonitrile	tetrahydrofuran	methyl *tert*-butyl ether	*tert*-butyl acetate	water
1	5.7 ± 1.0	10 ± 1	9.4 ± 1.2	20 ± 2	28 ± 2
1·chloroacetic acid	4.8 ± 1.1[b]				
1·benzoic acid	24 ± 1[b]				27 ± 2[b]
1·3,4,5-trimethoxycinnamic acid	38 ± 2[b]	40 ± 2[b]	37 ± 3[b]	> 50[b,c]	28 ± 1[b]

[a] The conditions for the transesterification reaction were the following: 40 mM racemic **1**, 200 mM propanol, 10 mg/mL CLC lipase, and shaking at 30 °C and 300 rpm. For the hydrolysis reaction (the last column), the conditions were the following: 10 mM aqueous phosphate buffer (pH 7.0), 10 mM racemic **1**, 0.2 mg/mL enzyme, and shaking at 4 °C and 300 rpm. Under these conditions, no appreciable reaction was detected without enzyme in any of the solvents. The enantioselectivity *E*, defined as $(k_{cat}/K_M)_S/(k_{cat}/K_M)_R$, was measured by means of chiral HPLC with Chiralcel OD-H (for transesterification) or Crownpak CR-(+) (for hydrolysis) columns. The *E* values presented are the mean values obtained from at least three independent measurements, with the standard deviations indicated. The salts were obtained by mixing **1** and the corresponding acid in water (pH 7.0), followed by extraction with ethyl acetate, rotary evaporation of the solvent, and subsequent redissolution in one of the solvents listed in the table. For other experimental conditions, see Methods. [b] The initial reaction rate for the faster (*S*) enantiomer of **1** decreased due to salt formation by 40%, 32%, and 46% in acetonitrile (for the salts given in the table order), and by 53%, 43%, and 50% for the 3,4,5-trimethoxycinnamic salt in tetrahydrofuran, methyl *tert*-butyl ether, and *tert*-butyl acetate, respectively. There was no appreciable rate reduction in water. [c] Estimated based on the detection limit of our chiral HPLC technique.

Scheme 1

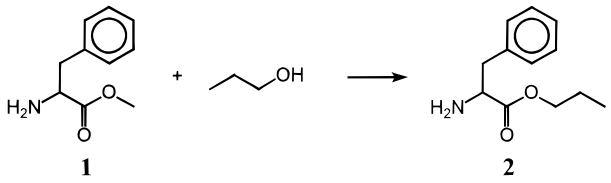

1 **2**

enzyme toward a given substrate. In doing so, as mentioned in the Introduction, we take advantage of the opportunities stemming from conducting enzymatic resolutions in organic solvents instead of water.

When one substrate enantiomer is preferred by an enzyme over the other, it means that the Gibbs free energy of the former's enzyme-bound transition state $G^{\ddagger}$ is lower than that of the latter. In the simplest case, this difference in the free energies is due to greater encumbrances suffered by the less reactive enantiomer in the enzyme active site. If so, then complexing the substrate with a bulky agent should exaggerate these steric difficulties (presumably to a larger extent than for the more reactive enantiomer), disparately raise the $G^{\ddagger}$ values, and thus increase enzymatic enantioselectivity. In the present work, we explored and validated this rationale by forming salts between various substrates and suitable Brønsted−Lowry acids or bases. Note that in contrast to covalent modifications of the substrate, a salt can be readily decomposed to regenerate the free reactants.

The first asymmetric transformation examined by us herein was enzymatic transesterification of phenylalanine methyl ester (**1**) depicted in Scheme 1. Initially, we employed cross-linked crystalline (CLC) enzymes as catalysts[11] because their structure in organic solvents has been shown to be essentially native[12] (unlike that of lyophilized enzymes[13]), and it was our intention in this study to perform structure-based computer modeling of enzyme-bound transition states of chiral substrates such as **1**.

Of the four different CLC enzymes tested by us as catalysts of the propanolysis of **1** in anhydrous acetonitrile, namely bovine pancreatic γ-chymotrypsin, subtilisin Carlsberg, and lipases from *Candida rugosa* and *Pseudomonas cepacia*,[14] the proteases were too enantioselective ($E > 50$) to be accurately assayed using our methodology, and the first lipase was unreactive. On the other hand, *P. cepacia* lipase was found to be both reasonably reactive and enantioselective not only in acetonitrile but also in other solvents, both organic and aqueous, with *E* values varying from 5 to 30 (first line in Table 1).

The *E* value of 5.7 observed in acetonitrile (Table 1), while clearly reflecting the enzyme's preference for the *S* enantiomer of **1**, would be insufficient for an effective resolution of the racemate. Therefore we endeavored to improve it by using the rationale outlined above. Specifically, a salt was formed between the amino group of **1** and the carboxyl group of a common organic acid, benzoic acid.[16] This salt was then subjected to the enzymatic transesterification (Scheme 1) in acetonitrile under the same conditions as the free **1**. While the reactivity of the more reactive, *S* enantiomer upon salt formation with benzoic acid decreased by less than a third, that of the *R* enantiomer slumped, thereby resulting in more than a 4-fold jump in the *E* (Table 1).

It was interesting to examine how the *E* value of a **1** salt depends on the size of the Brønsted−Lowry acid. To this end, we selected one carboxylic acid smaller (chloroacetic), and another larger (3,4,5-trimethoxycinnamic), than benzoic. The data presented in the first column of Table 1 show that the bulkier the counterion, the greater the enzymatic enantioselectivity with the resultant **1** salt. The highest enantioselectivity, $E = 38$, was observed with the salt of 3,4,5-trimethoxycinnamic acid whose *S* enantiomer was still more than half as reactive as that of **1**, while the reactivity of the *R* enantiomer plummeted almost 12-fold compared to that of the free base.

To obtain further insights into why *P. cepacia* lipase is more enantioselective toward the salts of **1** than toward the free substrate (Table 1), we employed the means of molecular modeling involving molecular dynamics, energy minimization, and van der Waals surface calculations.[15] The structure of the enzyme-bound transition state of **1** in the propanolysis reaction depicted in Scheme 1, approximated by the corresponding tetrahedral intermediate (see Methods), was built from the

(11) Margolin, A. L. *Trends Biotechnol.* **1996**, *18*, 223−230.

(12) Fitzpatrick, P. A.; Steinmetz, A. C. U.; Ringe, D.; Klibanov, A. M. *Proc. Natl. Acad. Sci. U.S.A.* **1993**, *90*, 8653−8657. Fitzpatrick, P. A.; Ringe, D.; Klibanov, A. M. *Biochem. Biophys. Res. Commun.* **1994**, *198*, 675−681. Schmitke, J. L.; Stern, L. J.; Klibanov, A. M. *Proc. Natl. Acad. Sci. U.S.A.* **1997**, *94*, 4250−4255. Schmitke, J. L.; Stern, L. J.; Klibanov, A. M. *Proc. Natl. Acad. Sci. U.S.A.* **1998**, *95*, 12918−12923.

(13) Griebenow, K.; Klibanov, A. M. *Proc. Natl. Acad. Sci. U.S.A.* **1995**, *92*, 10969−10976.

(14) Chymotrypsin was crystallized and cross-linked by us as described previously.[15] The other three cross-linked crystalline enzymes, commercially available from Altus Biologics, Inc., were generously donated by that company.

(15) Ke, T.; Wescott, C. R.; Klibanov, A. M. *J. Am. Chem. Soc.* **1996**, *118*, 3366−3374. Ke, T.; Klibanov, A. M. *J. Am. Chem. Soc.* **1998**, *120*, 4259−4263.

(16) The structure of all Brønsted−Lowry salts examined in this work was confirmed by FTIR spectroscopy, as described in the Methods section.

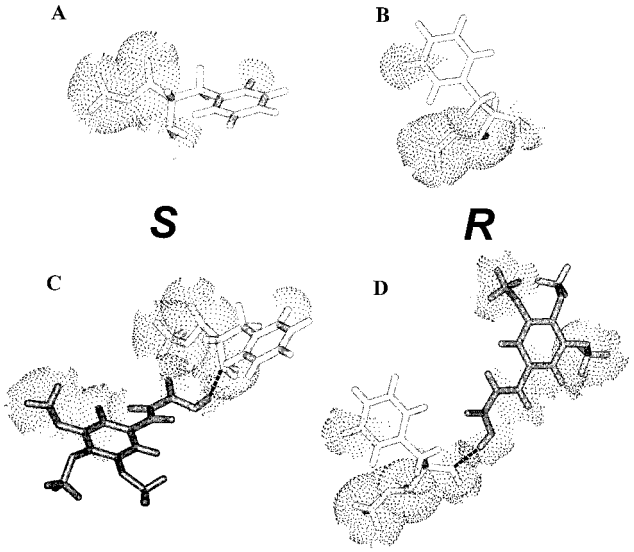

Figure 1. Molecular models of the enzyme-bound transition states of *S*-**1** (A) and *R*-**1** (B), as well as of their 3,4,5-trimethoxycinnamic acid salts (C and D, respectively). The transition states, approximated by the relevant tetrahedral intermediates, correspond to the acylation phase of the transesterification reaction depicted in Scheme 1 catalyzed by *Pseudomonas cepacia* lipase. The molecular models were built on the basis of the X-ray crystal structure of the lipase with use of molecular dynamics, energy minimization, and van der Waals surface calculations, as described in the Methods section. For clarity, only the substrate portions of the transition states are shown; the position of the enzyme is identically fixed in all instances (A through D). The dots correspond to the van der Waals surfaces of the substrate transition states that overlap with those of the enzyme. In C and D, the darkened structures represent the 3,4,5-trimethoxycinnamic counterion of the salt, and the dashed lines represent the putative salt bridge between the counterion and **1**.

recently published crystal structure of the enzyme.[17] Figure 1 shows such transition-state structures for the *S* and *R* enantiomers of **1** (A and B, respectively). The dotted surfaces are the parts of the substrate transition states that overlap with the enzyme. Figures 1C and 1D show such structures deduced for the enantiomers of the salt of **1** and 3,4,5-trimethoxycinnamic acid (the darkened fragment). One can see that the counterion in the *R* transition state (Figure 1D) has a greater surface overlap with the enzyme (i.e., greater steric hindrances) than the *S* enantiomer.

Similar molecular models were generated for the other salts listed in Table 1, and the calculated areas of the surface overlap (ASO) for both free **1** and its salts are presented in Table 2. These data show quantitatively that there is a correlation between the lipase enantioselectivity and the difference in the ASO between the two enantiomers (the last column in Table 2).

To ensure that the observed enhancement of the lipase enantioselectivity toward **1** due to salt formation is not limited to a single reaction medium, we examined this effect in additional anhydrous solvents. It is seen in Table 1 that 3,4,5-trimethoxycinnamic acid, which afforded the greatest *E* enhancement in acetonitrile, also increases several-fold the enzymatic enantioselectivity in tetrahydrofuran, methyl *tert*-butyl ether, and *tert*-butyl acetate. In contrast, there is *no* enantioselectivity enhancement (or rate changes) in water (the last column in Table 1), presumably because the salts dissociate in aqueous solution, and hence the chemical species reacting with the enzyme is the protonated **1** regardless of whether its initial form is the free base or a salt (such a dissociation should not occur in organic solvents).

Table 2. Comparison of the Experimentally Determined Enantioselectivities of Cross-linked Crystalline *Pseudomonas cepacia* Lipase toward **1** and Its Salts with Molecular Modeling Data[a]

		area of surface overlap (ASO),[b] Å^2		
substrate	*E* (*S*/*R*)	*S*	*R*	*R*−*S*
1	5.7 ± 1.0	40.1	45.4	5.3
1·chloroacetic acid	4.8 ± 1.1	45.6	51.4	5.8
1·benzoic acid	24 ± 1	50.9	63.7	12.8
1·3,4,5-trimethoxy-cinnamic acid	38 ± 2	63.7	78.1	14.4

[a] The *E* values are for the transesterification depicted in Scheme 1 in anhydrous acetonitrile. The molecular modeling (Figure 1) data include the areas of the van der Waals surfaces of the substrate transition states that overlap with those of the enzyme, as well as the difference in that parameter between the *R* and *S* enantiomers. The *E* values are taken from the first column of Table 1. The ASO values were calculated by using the following protocol: (i) molecular models of the transition state of the enzyme-bound substrate were constructed for both **1** and its salts; (ii) using the models, the ASO for each enantiomer of the substrate was derived from the difference in the van der Waals surfaces between its unbound and enzyme-bound states. For details, see Methods. [b] In addition to the ASO values, we also calculated the $\Delta\Delta G^{\ddagger}$ values between the *S* and *R* transition state models. In the order in the table, they were −0.36, −0.10, −1.37, and −1.24 kcal/mol. Comparison of these numbers with the experimental $\Delta\Delta G^{\ddagger}$ values derived from the *E* values in the table (−1.05, −0.94, −1.91, and −2.18 kcal/mol) revealed only a qualitative agreement in terms of the overall trend: there was an unexplainable systematic upward shift in all the calculated values. Therefore, we adopted the ASO as the means to rationalize the effect of salt formation on enzymatic enantioselectivity.

While we used crystalline *P. cepacia* lipase to catalyze the transesterification of **1** (to know the enzyme structure and thus be able to carry out molecular modeling depicted in Figure 1), lyophilized enzymes are still most frequently used as catalysts in organic solvents.[7] Upon lyophilization, the enzyme structure usually (reversibly) changes,[13] giving rise to altered enantioselectivity when assayed in organic solvents[9,15] (in water, the reversibly denatured conformation reverts back to the native). We found that the enantioselectivity of lyophilized lipase in the reaction shown in Scheme 1 in acetonitrile is 3.2 ± 0.9, i.e., lower than that of its CLC counterpart. However, this *E* value can be improved to 7.8 ± 1.1 by forming the salt of **1** with 3,4,5-trimethoxycinnamic acid.

The salts of **1** listed in Table 1 were preformed in water, extracted with ethyl acetate, and then dissolved in one of the solvents following rotary evaporation of the ethyl acetate (see Methods for details). Alternatively, a salt can be prepared directly in the solvent of interest by mixing **1** and a desired acid, followed by a 15-min refluxing. This simpler procedure gave the same result in terms of both the structure of the salt formed[16] and the enhanced *E* value obtained (36 ± 2 *vs* 38 ± 2).

It was essential to ascertain the generality of the proposed approach to enhancing enzymatic enantioselectivity with respect to the substrate. To this end, we selected another substrate, tropic acid (**3**); the *S* enantiomers of its many derivatives are potent anti-cholinergic drugs.[18] In addition to being structurally distinct from **1**, **3** acted as a Brønsted−Lowry acid (instead of a base) in the salt formation and as a nucleophile (instead of an acyl donor) in an enzymatic transesterification (Scheme 2).

(17) Schrag, J. D.; Li, Y.; Cygler, M.; Lang, D.; Burgdorf, T.; Hecht, H.-J.; Schmid, R.; Schomburg, D.; Rydel, T. J.; Oliver, J. D.; Strickland, L. C.; Dunaway, C. M.; Larson, S. B.; Day, J.; McPherson, A. *Structure* **1997**, *5*, 187−202.

(18) These include atropine, hyoscyamine, and scopolamine (Reynolds, J. E. F., Ed. *Martindale, the Extra Pharmacopoeia*, 28th ed.; Pharmaceutical Press: London, 1982; p 304).

Scheme 2

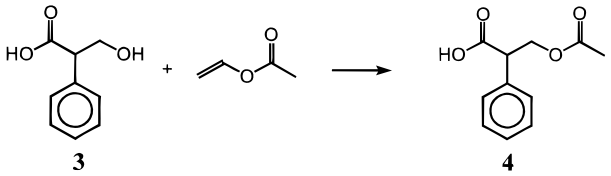

Table 3. Enantioselectivity of Cross-linked Crystalline *Pseudomonas cepacia* Lipase toward **3** and Its Salts with Various Amines in the Transesterification Depicted in Scheme 2 in Different Anhydrous Solvents[a]

	E (*R*/*S*)		
substrate	acetonitrile	tetrahydrofuran	toluene
3	1.1 ± 0.1	1.0 ± 0.2	1.6 ± 0.1
3·tetrabutylammonium	2.4 ± 0.2[b]		
3·tribenzylamine	3.5 ± 0.3[b]		
3·3,5-lutidine	3.8 ± 0.3[b]		
3·isoquinoline	4.2 ± 0.4[b]		
3·4-phenylpyridine	5.8 ± 0.4[b]		
3·1-adamantanamine	5.9 ± 0.4[b]		
3·quinuclidine	7.0 ± 0.6[b]	7.6 ± 0.5[b]	6.2 ± 0.5[b]

[a] The conditions for the transesterification reactions were the following: 40 mM racemic **3**, 200 mM vinyl acetate, 2 mg/mL CLC lipase, and shaking at 30 °C and 300 rpm. Under these conditions, no appreciable reaction was detected without enzyme in any of the solvents. The enantioselectivity *E*, defined as $(k_{cat}/K_M)_R/(k_{cat}/K_M)_S$, was measured by means of chiral HPLC with a Chiralcel OD-H column. The *E* values presented are the mean values obtained from at least two independent measurements, with the errors indicated. The salts were obtained by mixing **3** and the corresponding equimolar amine in acetonitrile, followed by a 15-min refluxing, rotary evaporation of the solvent, and subsequent redissolution of the salt in one of the solvents listed in the table. For other experimental conditions, see Methods. [b] The initial reaction rate for the faster (*R*) enantiomer of **3** decreased due to salt formation by 72%, 83%, 23%, 34%, 41%, 43%, and 35% in acetonitrile (for the salts given in the table order), and by 33% and 39% for the quinuclidine salts in tetrahydrofuran and toluene, respectively.

P. cepacia lipase exhibited no appreciable enantioselectivity in the acylation of **3** with vinyl acetate in acetonitrile ($E = 1.1 \pm 0.1$, Table 3).[19] We attempted to make the enzyme enantioselective toward **3** by using the substrate's carboxyl group to form salts with tertiary and quaternary amines. The data obtained for seven such amines of diverse structures are presented in the first column of Table 3. One can see that while all of them cause the lipase to prefer the *R* enantiomer of the substrate, the magnitude of the effect is strongly influenced by the nature of the base. Bulky but flexible tetrabutylammonium and tribenzylamine afford only modest *E* values (2.4 and 3.5, respectively). Among structurally rigid amines, the enantioselectivity enhancement grows with size to reach 7.0 for quinuclidine, which is quite impressive given enzyme's lack of enantiopreference for free **3**.

As with **1** (Figure 1), molecular modeling was employed to rationalize these observations. One can see in Figure 2 (parts A and B) and in the first line of Table 4 that the lipase-bound *R* and *S* transition states of **3** have very similar areas of surface overlap, which is evidently responsible for the absence of enantioselectivity. The situation is conspicuously different with the quinuclidine salts, where the counterion in the more reactive *R* enantiomer (Figure 2C) is enveloped with far fewer dots than the *S* one (Figure 2D); the quantitative ASO data (the last line in Table 4) support these visual impressions. In addition, for all the salts examined there is a correlation between the observed

(19) Subtilisin and *C. rugosa* lipase were found to be catalytically inactive in this reaction, while chymotrypsin was both active and very enantioselective ($E = 12.2 \pm 0.2$).

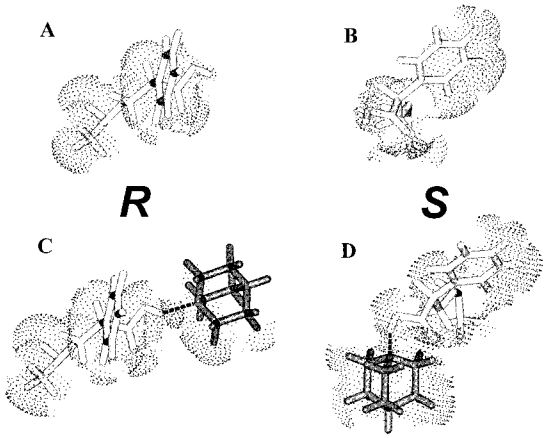

Figure 2. Molecular models of the enzyme-bound transition states of *R*-**2** (A) and *S*-**2** (B), as well as of their quinuclidine salts (C and D, respectively). The transition states correspond to the deacylation phase of the transesterification reaction depicted in Scheme 2 catalyzed by *Pseudomonas cepacia* lipase. For other details, see the legend to Figure 1 (with quinuclidine being the counterion).

Table 4. Comparison of the Experimentally Determined Enantioselectivities of Cross-linked Crystalline *Pseudomonas cepacia* Lipase toward **3** and Its Salts with Molecular Modeling Data[a]

		area of surface overlap (ASO), Å^2		
substrate	*E* (*R*/*S*)	*R*	*S*	*S*−*R*
3	1.1 ± 0.1	42.3	42.9	0.6
3·tetrabutylammonium	2.4 ± 0.2	70.1	73.1	3.0
3·tribenzylamine	3.5 ± 0.3	76.2	79.6	3.4
3·3,5-lutidine	3.8 ± 0.3	54.5	61.4	6.9
3·isoquinoline	4.2 ± 0.4	53.2	60.8	7.5
3·4-phenylpyridine	5.8 ± 0.4	55.6	63.5	7.9
3·1-adamantanamine	5.9 ± 0.4	58.4	66.2	7.8
3·quinuclidine	7.0 ± 0.6	57.6	67.0	9.3

[a] The *E* values are for the transesterification depicted in Scheme 2 in anhydrous acetonitrile. The molecular modeling (Figure 2) data include the areas of the van der Waals surfaces of the substrate transition states that overlap with those of the enzyme, as well as the difference in that parameter between the *S* and *R* enantiomers. The *E* values were taken from the first column of Table 3. See footnotes to Table 2 and Methods for more details.

E and ΔASO ($ASO_S - ASO_R$) (the first and last columns in Table 4)—the greater the steric hindrances endured disproportionately by the less reactive enantiomer, the greater the enzymatic enantioselectivity.

As in the case of **1**, the enhancement of enantioselectivity brought about by salt formation of **3** was manifested in various solvents: the *E* rose from 1.0 to 7.6 in tetrahydrofuran and from 1.6 to 6.2 in toluene upon transition from free **3** to its quinuclidine salt (Table 3). The results obtained with different modes of salt formation and with lyophilized (rather than crystalline) *P. cepacia* lipase also resembled those with **1**. The quinuclidine salt of **3** preformed in water, followed by extraction (rather than by direct mixing in the nonaqueous solvent, followed by refluxing, as in Table 3), gave the *E* value of 6.8 ± 0.7 in acetonitrile. Likewise, the enantioselectivity of the lyophilized lipase in that solvent rose from 1.3 ± 0.1 for the free substrate to 4.8 ± 0.4 for its quinuclidine salt.

To verify the generality of our strategy further, we next extended its scope not only to another, dissimilar substrate but also to a distinct type of a reaction catalyzed by a different enzyme. Specifically, we examine the hydrolysis (instead of transesterification) of 2-benzylsuccinic acid 1-monomethyl ester (**5**) catalyzed by the CLC protease subtilisin Carlsberg (instead

Table 5. Enantioselectivity of Cross-linked Crystalline Subtilisin Carlsberg toward **5** and Its Salts with Various Amines in the Hydrolysis Depicted in Scheme 3 in Different Organic Solvents Containing 1% Water and in Water[a]

	E (*S*/*R*)					
substrate	*tert*-amyl alcohol	methyl *tert*-butyl ether	acetonitrile	*tert*-butanol	2-propanol	water
5	1.5 ± 0.1	2.0 ± 0.1	1.8 ± 0.1	2.0 ± 0.2	2.1 ± 0.2	9.8 ± 0.9
5·3,5-lutidine	2.8 ± 0.2[b]					
5·isoquinoline	3.1 ± 0.3[b]					
5·quinuclidine	3.6 ± 0.3[b]					
5·1-adamantanamine	4.3 ± 0.4[b]					
5·4-phenylpyridine	6.9 ± 0.5[b]	5.9 ± 0.4[b]	7.3 ± 0.6[b]			
5·4-(4-chlorobenzoyl)pyridine	8.1 ± 0.6[b]	7.0 ± 0.5[b]	7.8 ± 0.5[b]	8.4 ± 0.7[b]	6.5 ± 0.5[b]	9.6 ± 0.6[b]

[a] The conditions for the hydrolysis reaction in organic solvents were the following: 40 mM racemic **5**, 1% (v/v) water, 10 mg/mL CLC subtilisin, and shaking at 30 °C and 300 rpm. For the hydrolysis reaction in water (the last column), the conditions were the following: 10 mM aqueous phosphate buffer (pH 7.0), 10 mM racemic **5**, 0.4 mg/mL enzyme, and shaking at 4 °C and 300 rpm. Under these conditions, no appreciable reaction was detected without enzyme in any of the solvents. The enantioselectivity *E*, defined as $(k_{cat}/K_M)_S/(k_{cat}/K_M)_R$, was measured by means of chiral HPLC with a Chiralcel OD-H column. The *E* values presented are the mean values obtained from at least three independent measurements, with the standard deviations indicated. The salts were obtained by mixing **5** and the corresponding equimolar amine in acetonitrile, followed by a 15-min refluxing, rotary evaporation of the solvent, and subsequent redissolution of the salt in one of the solvents listed in the table. For other experimental conditions, see Methods. [b] The initial reaction rate for the faster (*S*) enantiomer of **5** decreased due to salt formation by 32%, 41%, 28%, 34%, 41%, and 55% in *tert*-amyl alcohol (for the salts given in the table order), by 33% and 39% for the 4-phenylpyridine salt in methyl *tert*-butyl ether and acetonitrile, respectively, and by 53%, 45%, 60%, and 61% for the 4-(4-chlorobenzoyl)pyridine salt in methyl *tert*-butyl ether, acetonitrile, *tert*-butanol, and 2-propanol, respectively. There was no detectable rate reduction in water.

Scheme 3

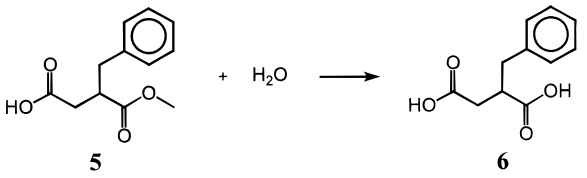

of *P. cepacia* lipase) as shown in Scheme 3. The enantioselectivity in this reaction carried out in *tert*-amyl alcohol containing 1% water (to allow hydrolysis) was 1.5 (Table 5), i.e., subtilisin exhibited a slight preference for *S*-**5**.

Six tertiary amines, either from Table 3 or new, were selected as salt-forming bases with the carboxyl group of **5** and hence as potential *E*-enhancing agents. The data obtained, presented in Table 5, reveal that all of them indeed raise subtilisin's enantioselectivity, with, e.g., 4-(4-chlorobenzoyl)pyridine exerting more than a 5-fold effect. Note that the order of the amines in terms of their enantioselectivity enhancement in Table 5 is distinct from that in Table 3: for example, quinuclidine, which was the most potent agent with **3**, is in the bottom half with **5**. Molecular modeling (Figure 3) proved insightful in explaining this trend. As can be seen in Table 6, the order of the ascending *E* values unmistakably correlates with the order of the increasing ΔASO values.

Inspection of Table 5 reveals that, as with **1** and **3**, salts of **5** are better enantiodifferentiated enzymatically than the free substrate in a variety of organic solvents (all containing 1% water). On the other hand, as with **1** (Table 1), in water the enzymatic enantioselectivity against even the 4-(4-chlorobenzoyl)pyridine salt was the same as that against the free **5**.

The observed enzymatic enantioselectivity against a given substrate salt was, once again, independent of how the latter was prepared—whether via direct mixing in a solvent followed by refluxing (Table 5), or via formation in water followed by extraction. Likewise, the enantioselectivity of lyophilized subtilisin toward **5** in *tert*-amyl alcohol was raised by forming the 4-(4-chlorobenzoyl)pyridine salt (from 1.7 ± 0.1 to 5.2 ± 0.4), although to a lesser extent than in the case of the CLC enzyme (Table 5).

To illustrate the synthetic utility of our enantioselectivity enhancement strategy, we carried out preparative resolution of racemic **3** catalyzed by *P. cepacia* lipase. When the free acid

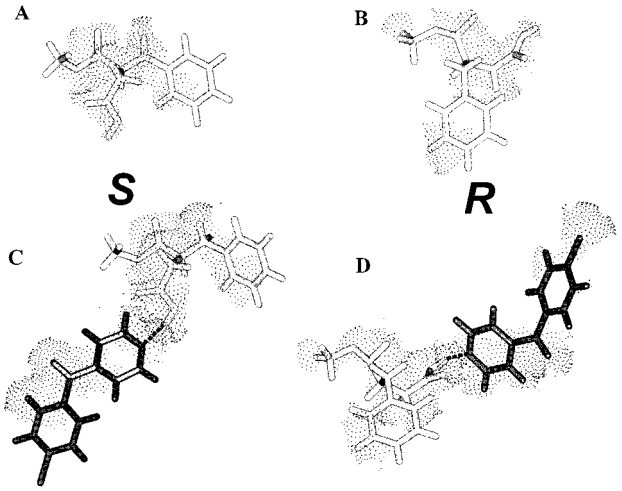

Figure 3. Molecular models of the enzyme-bound transition states of *S*-**3** (A) and *R*-**3** (B), as well as of their 4-(4-chlorobenzoyl)pyridine salts (C and D, respectively). The transition states correspond to the acylation phase of the hydrolysis reaction depicted in Scheme 3 catalyzed by the protease subtilisin Carlsberg. For other details, see the legend to Figure 1 (with 4-(4-chlorobenzoyl)pyridine being the counterion).

was enzymatically acetylated (Scheme 2) in acetonitrile,[20] the e.e. value of the acetyl-**3** obtained after a 35% conversion was an insignificant 6%. However, when the resolution was conducted with the quinuclidine salt of **3** under otherwise the same conditions, the e.e. of the resultant acetyl-**3** was a much more impressive 65%.

In closing, in this study we proposed a new approach to making a given enzyme more enantioselective in organic solvents toward a given substrate, with no covalent alterations, by converting the latter into a readily reversible salt. This approach was validated by using several structurally diverse substrates, salt-forming Brønsted−Lowry acids and bases, and

(20) In 30 mL of anhydrous acetonitrile, 1.2 mmol of *R*,*S*-**3** (or its quinuclidine salt) and 6 mmol of vinyl acetate were dissolved. The enzymatic acetylation was initiated by adding 60 mg of CLC *P. cepacia* lipase. The reaction mixture was shaken at 300 rpm and 30 °C for 8.3 h (free substrate) or 12.1 h (substrate salt). Then the enzyme was removed by filtration, and the remaining solution was worked up by rotary evaporation, redissolution in 60% ethyl acetate/40% hexane/0.1% trifluoroacetic acid (which decomposes the salt), and using this solvent as a mobile phase in flash silica gel column chromatography (see Methods for details).

Table 6. Comparison of the Experimentally Determined Enantioselectivities of Cross-linked Crystalline Subtilisin Carlsberg toward **5** and Its Salts with Molecular Modeling Data[a]

substrate	*E* (*S*/*R*)	area of surface overlap (ASO), Å^2		
		S	*R*	*R*−*S*
5	1.5 ± 0.1	27.0	27.9	0.9
5·3,5-lutidine	2.8 ± 0.2	34.3	36.8	2.5
5·isoquinoline	3.1 ± 0.3	40.1	43.1	3.0
5·quinuclidine	3.6 ± 0.3	36.3	40.6	4.3
5·1-adamantanamine	4.3 ± 0.4	39.8	44.2	4.4
5·4-phenylpyridine	6.9 ± 0.5	42.5	47.4	4.9
5·4-(4-chlorobenzoyl)-pyridine	8.1 ± 0.6	45.3	50.7	5.4

[a] The *E* values are for the hydrolysis depicted in Scheme 3 in *tert*-amyl alcohol containing 1% water. The molecular modeling (Figure 3) data include the areas of the van der Waals surfaces of the substrate transition states that overlap with those of the enzyme, as well as the difference in that parameter between the *R* and *S* enantiomers. The *E* values were taken from the first column of Table 5. For more details, see footnotes to Table 2 and Methods.

solvents, as well as different enzymes and reactions catalyzed by them. The results suggest that, at least for the instances examined, the steric hindrances suffered by the less reactive substrate enantiomer in the enzyme-bound transition state are the predominant reason for enzymatic enantiodiscrimination; when these hindrances are exacerbated further by enlarging the substrate due to salt formation, the enantioselectivity rises. It is also clear that the substrate salts remain intact even in the enzyme-active sites. Molecular modeling of *R* and *S* enzyme-bound transition states, for both the free substrates and their various salts, reveals a surprisingly good correlation in each substrate series between experimentally determined *E* values and the calculated differential areas of surface overlap (ASO for the less reactive enantiomer minus that for the more reactive one). The proposed enantioselectivity enhancement strategy is effective in organic solvents but *not* in water (where the salts evidently dissociate thus reverting to the free substrates). Thus the present work points to novel synthetic opportunities afforded by nonaqueous enzymatic catalysis. In addition to the salt formation explored herein, these presumably may also include other reversible complexes stable in organic solvents but not in water.

Materials and Methods

Enzymes. Cross-linked crystals of *P. cepacia* lipase, *C. rugosa* lipase, and subtilisin Carlsberg were gifts from Altus Biologics, Inc. γ-Chymotrypsin was crystallized and cross-linked with glutaraldehyde using the previously described procedure.[15] Prior to use, enzyme crystals were filtered, washed twice with dry acetonitrile and then twice with the corresponding solvent.

Lyophilized enzyme powders were prepared as follows: the enzyme was dissolved (5 mg/mL) in 20 mM aqueous phosphate buffer of pH 7.0 or 7.8 (for *P. cepacia* lipase and subtilisin Carlsberg, respectively) at 4 °C, then the solution was frozen using liquid N_2, and lyophilized for 48 h.

Chemicals and Solvents. Most of the chemicals and solvents used in this work were purchased from Aldrich Chemical Co. and Sigma Chemical Co. *R*- and *S*-**5** were from Chirotech Technology Ltd., and (±)-**6** was from Narchem Corp. Organic solvents were of the highest purity available from Aldrich (analytical grade or better) and were dried prior to use by shaking with Linde's 3-Å molecular sieves.

(±)-**1** was prepared by dissolving 1.0 g of its hydrochloride in 40 mL of deionized water and adjusting the pH to 10. This solution was extracted with 50 mL of ethyl acetate thrice, followed by combining the organic layers and drying over anhydrous $MgSO_4$. Subsequent rotary evaporation resulted in 0.74 g of (±)-**1** (90% of theoretical yield). *R*-**1** was prepared the same way (to determine the elution sequence of the enantiomers in chiral HPLC). Using a mobile phase of 99% hexane/1% 2-propanol/0.1% diethylamine (henceforth, all such percentages are v/v/v) with a flow rate of 0.80 mL/min and a Chiralcel OD-H column, *R*- and *S*-**1** were separated with retention times of 34.4 and 38.6 min, respectively.

Racemic **2** was synthesized[21] by dissolving 200 mg of (±)-phenylalanine in 20 mL of anhydrous propanol, followed by refluxing with simultaneous purging with dry HCl gas. The resulting reaction mixture was concentrated in a vacuum and cooled, and the crystals were filtered off and recrystallized from propanol (yield of 130 mg, 60% of theoretical). ^{1}H NMR ($CDCl_3$) δ 7.37 (5H, m), δ 4.20 (1H, m), 3.84 (2H, t, J = 7.2 Hz), 3.30 (1H, dd, J = 6.2, 11.5 Hz), 3.19 (1H, dd, J = 4.6, 11.4 Hz), 1.64 (2H, m), 7.3 (3H, t, J = 7.7 Hz). To determine the elution sequence of the enantiomers, *R*-**2** was synthesized the same way except for using *R*-Phe as a starting material. Using the same chiral HPLC conditions as for **1**, *R*- and *S*-**2** had retention times of 23.2 and 25.6 min, respectively.

Using the procedure of McKenzie and Wood,[22] (±)-**3** was recrystallized three times with equimolar quinine in ethanol to give *R*-**3** with an e.e. of 96%, as determined by chiral HPLC. Using a mobile phase of 96% hexane/4% 2-propanol/0.1% trifluroacetic acid with a flow rate of 0.50 mL/min and a Chiralcel OD-H column, *R*- and *S*-**3** had retention times of 40.7 and 46.0 min, respectively.

Racemic **4** was synthesized[23] by dissolving 250 mg of (±)-**3** in 20 mL of dry tetrahydrofuran, and 200 mg of acetyl chloride was added dropwise at 4 °C. The resulting reaction mixture was stirred at room temperature overnight and then quenched by addition of 20 mL of water. After extraction with ethyl acetate three times, the product was dried over $MgSO_4$, concentrated by rotary evaporation, and purified by flash silica gel column chromatography (yield of 213 mg, 68% of theoretical). ^{1}H NMR ($CDCl_3$) δ 7.32 (5H, s), 4.57 (dd, 1H, J = 9.5, 10.9 Hz), 4.34 (dd, 1H, J = 9.5, 10.9 Hz), 3.95 (dd, 1H, J = 5.5, 9.5 Hz), 2.03 (s, 3H). *R*-**4** was prepared the same way from *R*-**3** in order to determine the HPLC elution sequence of **4**. Using the same chiral HPLC conditions as for **3**, *R*- and *S*-**4** had retention times of 22.6 and 20.5 min, respectively.

R-**4** was also prepared enzymatically from (±)-**3**·quinuclidine salt (formed by refluxing, as described below). The salt (3 mg, 1.20 mmol) and 520 mg of vinyl acetate (6 mmol) were dissolved in 30 mL of acetonitrile, followed by addition of 60 mg of CLC *P. cepacia* lipase. The reaction mixture was shaken at 30 °C and 300 rpm. Once the overall conversion reached 35% (12.1 h), as judged by chiral HPLC, the reaction was stopped by filtering off the enzyme, and the filtrate was concentrated by rotary evaporation. The residue was redissolved in a small amount of the mobile phase (60% ethyl acetate/40% hexane/0.1% trifluroacetic acid) to decompose the salt, purified with flash silica gel column chromatography, and yielded 75 mg of *R*-**4** (30% of theoretical yield, 65% e.e. as determined by chiral HPLC). ^{1}H NMR ($CDCl_3$) δ 7.34 (5H, s), 4.60 (dd, 1H, J = 9.5, 11.1 Hz), 4.37 (dd, 1H, J = 9.4, 11.0 Hz), 3.95 (dd, 1H, J = 5.5, 9.5 Hz), 2.06 (s, 3H). Using the same procedure, the acetylation of **3** was carried out for 8.4 h, which yielded 78 mg of *R*-**4** (32% of theoretical yield, 6% e.e. as determined by chiral HPLC). ^{1}H NMR ($CDCl_3$) δ 7.21 (5H, s), 4.61 (dd, 1H, J = 9.9, 11.4 Hz), 4.31 (dd, 1H, J = 9.3, 11.8 Hz), 3.90 (dd, 1H, J = 5.7, 9.2 Hz), 2.01 (s, 3H).

Using a mobile phase of 97.5% hexane/2.5% 2-propanol/0.1% trifluroacetic acid with a flow rate of 0.80 mL/min and a Chiralcel OD-H column, *R*-**5**, *S*-**5**, *R*-**6**, and *S*-**6** had retention times of 27.4, 32.3, 40.7, and 54.5 min, respectively.

Kinetic Measurements. In the propanolysis of **1** in anhydrous solvents (Scheme 1), 10 mg/mL of lipase, 40 mM racemic **1**, and 200 mM propanol were used, while for the hydrolysis of **1** in 10 mM aqueous phosphate buffer (pH 7.0), 10 mM racemic **1** and 0.2 mg/mL of enzyme were used. For the acetylation of **3** (Scheme 2), 2 mg/mL of lipase, 40 mM racemic **3**, and 200 mM vinyl acetate were used. In the hydrolysis of **5** in organic solvents (Scheme 3), 10 mg/mL of subtilisin, 40 mM racemic **5**, and 1% (v/v) of deionized water were

(21) Vanderhaeghe, H. *J. Pharm. Pharmacol.* **1954**, *6*, 57−59.
(22) McKenzie, A.; Wood, J. K. *J. Chem. Soc.* **1919**, 828−834.
(23) Wolffenstein, M. *Chem. Ber.* **1908**, *41*, 730−736. Schmidt, R. *J. Pharm. Sci.* **1968**, *57*, 443−452.

used, while for the hydrolysis of **5** in 10 mM aqueous phosphate buffer (pH 7.8), 0.4 mg/mL of enzyme and 40 mM racemic **5** were used. All kinetic experiments in organic solvents were carried out at 30 °C, while the hydrolysis reactions in water were carried out at 4 °C. All reaction mixtures were shaken at 300 rpm, and the blank reactions were monitored under identical conditions without enzyme (no appreciable reaction was ever detected).

Periodically, 25-μL aliquots were withdrawn from reaction mixtures and assayed by chiral HPLC with a UV detector tuned to 258 nm. A Chiralcel OD-H column was used for most separations, except that a Crownpak CR-(+) was used for the separation of *R*- and *S*-phenylalanines. In initial rate measurements, the product conversion never exceeded 15%. Because in the transesterifications (or hydrolyses) of racemates the *R* and *S* substrate enantiomers compete for the same population of the free enzyme, the ratio of their initial rates is equal to $(k_{cat}/K_M)_R/(k_{cat}/K_M)_S$,[24] i.e., to *E*.[9] Each measurement was carried out at least in duplicate, and the typical deviation from the mean did not exceed 15%.

FTIR Measurements. The salt formation between the substrates and the corresponding Brønsted−Lowry acids or bases was verified by FTIR spectroscopy.[25] Under identical conditions, the FTIR spectra of the salt, the substrate, and the corresponding Brønsted−Lowry acid or base were recorded. Upon salt formation, the IR absorbance peak at around 1740 cm^{-1} of the participating carboxyl group typically either disappeared completely or dropped at least 2−3-fold.[25] This is due to the disruption of the C═O bond caused by the C−O−H−N bond network formation.[25] In the case of pyridine derivatives as salt-forming agents (some entries in Tables 3 and 5), a small peak around 1640 cm^{-1} was also observed assigned to aromatic N−H stretching.[25c,e]

The FTIR measurements were carried out in a Nicolet Magna-IR System 550 optical bench as described previously.[13] Samples were prepared in acetonitrile the same way as in the corresponding kinetic measurements. For **5**, *tert*-amyl alcohol solutions were also examined and gave the spectra identical with those in acetonitrile. In all measurements, 100-μm spacers were used; blank solvents were used as a background.

Salt Preparation. Typically, substrate salts were prepared as follows: 50 mM substrate and the corresponding Brønsted−Lowry acid or base were dissolved in acetonitrile and the solution was refluxed for 15 min, cooled, concentrated by rotary evaporation, and dried under vacuum overnight. Certain salts were also prepared via an alternative, extraction procedure. For example, 50 mM **1** was dissolved in deionized water, and the pH was adjusted to 7.0 by adding a saturated aqueous solution of 3,4,5-trimethoxycinnamic acid. The resulting solution was extracted thrice with equal volumes of ethyl acetate whose layers were combined, dried over $MgSO_4$, and concentrated in a vacuum overnight. Similar procedures were carried out for the salts of **1** with benzoic and chloroacetic acids, **3** with quinuclidine, and **5** with 4-phenylpyridine. In all FTIR and kinetic experiments, the salts prepared with this method behave identically to those prepared via the direct mixing/refluxing method.

Structural Modeling. Molecular models were built by using the crystal structures of *P. cepacia* lipase (Brookhaven Data Bank entry 2LIP) in water[17] and of subtilisin Carlsberg in acetonitrile (Brookhaven Data Bank entry 1SCB).[12] The transition states for the enzymatic acylations and deacylations were approximated by the corresponding tetrahedral intermediates.[26] Such models were obtained by using the two-step procedure described previously[15] with minor modification. First, potential binding modes of each enantiomer of the substrate were generated by performing molecular dynamics simulations, followed by energy minimization. The carbonyl oxygen of the substrate was tethered to the oxyanion binding site by using a harmonic potential with a force constant selected to allow widely different conformations to be explored, while preventing the substrate from diffusing too far from the enzyme. This substrate binding mode search is necessary because the covalently bound tetrahedral intermediate is sufficiently sterically constrained that molecular dynamics simulations do not sample highly different conformations separated by large energetic barriers. Each substrate-binding mode thus identified was used as a template for creating an initial model of the tetrahedral intermediate. The low-energy conformation of each of these starting models was found by using molecular dynamics simulations and energy minimizations. The lowest-energy conformer of the tetrahedral intermediate was selected as the model of the transition state. In the case of modeling substrate salts, the salt-forming group (amino or carboxyl) in the corresponding Brønsted−Lowry acid or base was tethered to the vicinity of the substrate by using a harmonic potential (50 kcal/(mol·Å^2)). A salt bridge was approximated by a hydrogen bond between the substrate and the corresponding acid or base with the hydrogen bond length of 2.0 Å and bond angle of 180° used as starting positions.[27] Each salt was subjected to the same two-step procedure as above, and the final lowest-energy conformer was selected as the transition state model.

The area of surface overlap (ASO) was calculated as follows: (i) using the final conformation of the transition state model, the van der Waals surfaces of the substrate and its salt partner were calculated individually in the absence of enzyme using Connolly's method[28] with a probe size of 0 Å; (ii) the same operation was repeated with the enzyme-bound transition state of the substrate salt; and (iii) the ASO (Tables 2, 4, and 6) was calculated as the difference between the sum of the surface areas calculated in step (i) (no enzyme) and that calculated in step (ii) (for the enzyme-bound situation). This parameter was used as a measure of steric hindrances encountered by the substrate (or its salt) in the enzyme-bound transition state (similar to the previously used[29] number of close contacts).

Acknowledgment. This work was financially supported by the National Science Foundation (Grant No. BES-9712497).

JA984283V

(24) Fersht, A. *Enzyme Structure and Mechanism*, 2nd ed.; Freeman: New York, 1985; p 112. Wescott, C. R.; Klibanov, A. M. *J. Am. Chem. Soc.* **1993**, *115*, 1629−1631.

(25) (a) Barrow, G. M.; Yerger, E. A. *J. Am. Chem. Soc.* **1954**, *76*, 5211−5216. (b) Yerger, E. A.; Barrow, G. M. *J. Am. Chem. Soc.* **1955**, *77*, 4474−4478. (c) Barrow, G. M. *J. Am. Chem. Soc.* **1956**, *78*, 5802−5814. (d) Yerger, E. A.; Barrow, G. M. *J. Am. Chem. Soc.* **1955**, *77*, 6206−6207. (e) Johnson, S. L.; Rumon, K. A. *J. Phys. Chem.* **1965**, *69*, 74−85.

(26) Warshel, A.; Naray-Szabo, G.; Sussman, F.; Hwang, J.-K. *Biochemistry* **1989**, *28*, 3629−3635.

(27) Donohue, J. *J. Phys. Chem.* **1952**, *56*, 502−510. Fuller, W. *J. Phys. Chem.* **1959**, *63*, 1705−1717.

(28) Connolly, M. L. *Science* **1983**, *221*, 709−715.

(29) Fitzpatrick, P. A.; Ringe, D.; Klibanov, A. M. *Biotechnol. Bioeng.* **1992**, *40*, 735−740.